

Design, Synthesis and Pharmacological Evaluation of Novel Hsp90N-terminal Inhibitors Without Induction of Heat Shock Response

Peng Liu^{+, [a, c]} Xiangling Chen^{+, [b, c]} Jianming Zhu,^[a] Bo Li,^{*[a, c]} Zhaoqiang Chen,^[a, c] Guimin Wang,^[a, c] Haiguo Sun,^[a, c] Zhijian Xu,^[a, c] Zhixin Zhao,^[b] Chen Zhou,^[b] Chengying Xie,^{*[b, c]} Liguang Lou,^{*[b, c]} and Weiliang Zhu^{*[a, c, d]}

Heat shock protein 90 (Hsp90) is a potential oncogenic target. However, Hsp90 inhibitors in clinical trial induce heat shock response, resulting in drug resistance and inefficiency. In this study, we designed and synthesized a series of novel triazine derivatives (A1-26, B1-13, C1-23) as Hsp90 inhibitors. Compound A14 directly bound to Hsp90 in a different manner from traditional Hsp90 inhibitors, and degraded client proteins, but did not induce the concomitant activation of Hsp72. Importantly, A14 exhibited the most potent anti-proliferation ability

by inducing autophagy, with the IC₅₀ values of 0.1 μM and 0.4 μM in A549 and SK-BR-3 cell lines, respectively. The *in vivo* study demonstrated that A14 could induce autophagy and degrade Hsp90 client proteins in tumor tissues, and exhibit anti-tumor activity in A549 lung cancer xenografts. Therefore, the compound A14 with potent antitumor activity and unique pharmacological characteristics is a novel Hsp90 inhibitor for developing anticancer agent without heat shock response.

1. Introduction

Heat shock protein 90 (Hsp90) is an ATP-dependent and highly conserved molecular chaperone which is responsible for the activation, stabilization, and function of a diverse range of client proteins.^[1,2] The client proteins are protein kinases and transcription factors playing vital roles in the signal pathway of tumor growth and metastasis, which consist of transmembrane tyrosine kinase receptor HER2, EGFR, CDK4, cyclin D, AKT,

mutant p53, RAF-1 and hypoxia-inducible factor-1α (HIF-1α), and so on.^[3,4] Hsp90 is constitutively expressed at 2- to 10-fold higher levels in tumor cells compared to their normal counterparts, suggesting that it may be critically important for tumor cell growth and survival.^[5] Usually, the degree of Hsp90 inhibition in cancer cells is assessed through the degradation of client proteins (eg. HER2, EGFR).^[6,7]

The Hsp90 monomer includes three main domains, namely a conserved N-terminal domain (NTD), C-terminal domain (CTD) and middle domain (MD).^[8] NTD is an ATP/ADP binding site, which is closely related to the function of Hsp90. So far, there are 17 small molecular compounds into clinical trials, all of which are NTD inhibitors.^[9] The NTD inhibitors mainly include three categories, viz., geldanamycin (GM) and its derivatives,^[10] radicicol and its derivatives,^[11] and purine analogues^[12] (Figure 1). These NTD inhibitors have shown little clinical advantage because of the induction of heat shock response (HSR) by the inhibitors, which can result in antiapoptotic and chemoresistance. HSR is a cellular stress response mediated by heat shock factor-1 (HSF-1),^[13,14] which transcribes and up-regulates the main protein levels of Hsp90 and Hsp72. It's a big challenge to find a Hsp90 inhibitor that does not induce HSR.

With the aim of designing novel Hsp90 inhibitors, our group had discovered X66 (A1) as a novel inhibitor of Hsp90.^[15] Besides, A1 neither activates HSF-1 nor stimulates the transcription of heat shock proteins (HSPs), such as Hsp72 and Hsp27,^[16,17] both of which are anti-apoptotic and tumorigenic.^[18] But, its bioactivity, with IC₅₀ values of around 5 μM against human non-small cell lung cancer A549 and breast cancer SK-BR-3 cell lines, needs to be further improved. In order to discover more potent Hsp90 inhibitors without inducing heat shock response, 2-(3,5-dimethyl-1H-pyrazol-1-yl)-1,3,5-triazine was used as a basic scaffold in this study for designing novel

[a] Dr. P. Liu,⁺ Dr. J. Zhu, Dr. B. Li, Dr. Z. Chen, Dr. G. Wang, Dr. H. Sun, Dr. Z. Xu, Prof. W. Zhu
Key Laboratory of Receptor Research, Drug Discovery and Design Center, Shanghai Institute of Materia Medica, Chinese Academy of Sciences, 555 Zuchongzhi Road, Shanghai 201203, China
E-mail: wlzhu@simm.ac.cn
boli@simm.ac.cn

[b] Dr. X. Chen,⁺ Dr. Z. Zhao, Dr. C. Zhou, Dr. C. Xie, Prof. L. Lou
Division of Anti-Tumor Pharmacology, Shanghai Institute of Materia Medica, Chinese Academy of Sciences, 555 Zuchongzhi Road, Shanghai 201203, China
E-mail: xiechengying818@simm.ac.cn
lgou@mail.shnc.ac.cn

[c] Dr. P. Liu,⁺ Dr. X. Chen,⁺ Dr. B. Li, Dr. Z. Chen, Dr. G. Wang, Dr. H. Sun, Dr. Z. Xu, Dr. C. Xie, Prof. L. Lou, Prof. W. Zhu
University of Chinese Academy of Sciences, No.19 A Yuquan Road, Beijing 100049, China

[d] Prof. W. Zhu
Open Studio for Druggability Research of Marine Natural Products, Pilot National Laboratory for Marine Science and Technology (Qingdao), 1 Wenhai Road, Aoshanwei, Jimo, Qingdao, 266237, China

[⁺] These authors made equal contributions to this work.

Supporting information for this article is available on the WWW under <https://doi.org/10.1002/open.201900055>

©2019 The Authors. Published by Wiley-VCH Verlag GmbH & Co. KGaA.
This is an open access article under the terms of the Creative Commons Attribution Non-Commercial NoDerivs License, which permits use and distribution in any medium, provided the original work is properly cited, the use is non-commercial and no modifications or adaptations are made.

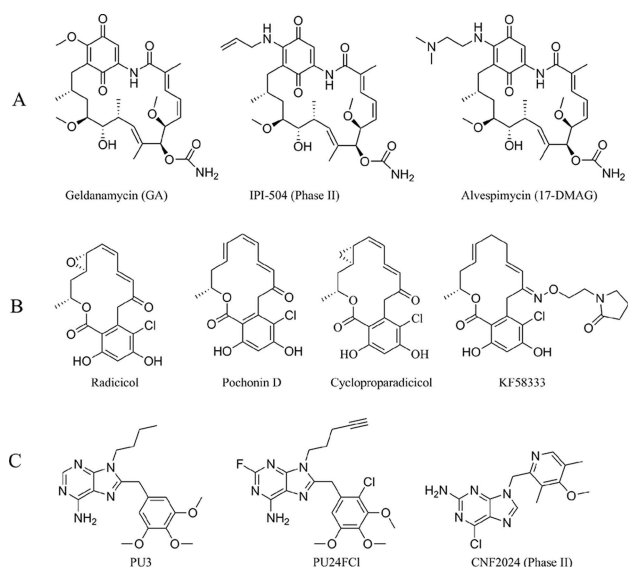


Figure 1. Examples of Hsp90 NTD inhibitors. (A) GM and its derivatives. (B) Radicicol and its derivatives. (C) Purine analogues.

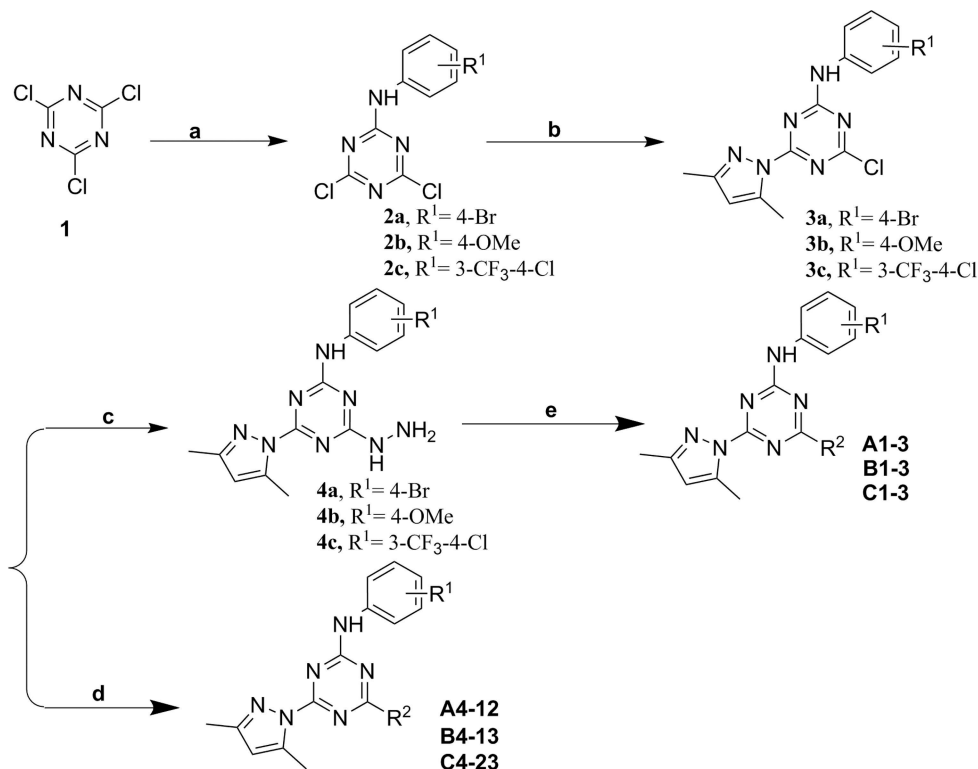
analogues. Accordingly, 61 new compounds were successfully synthesized. Bioassay of the newly synthesized triazine derivatives discovered potent Hsp90 inhibitors with anti-proliferative activity and the degradation of Hsp90 client proteins in tumor cells without heat shock response.

2. Results and Discussion

2.1 Chemistry

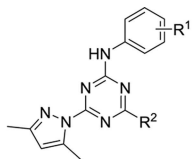
The general procedure for synthesis of compounds **A1-12**, **B1-13** and **C1-23** is elaborated in Scheme 1. 2,4,6-Trichloro-1,3,5-triazine (**1**) was reacted with amines (Table 1) to afford N-(4-bromophenyl)-4,6-dichloro-1,3,5-triazin-2-amine (**2a**). Then the chlorine atom at the 3-position of **2a** was substituted by 3,5-dimethyl-1H-pyrazole to give N-(4-bromophenyl)-4-chloro-6-(3,5-dimethyl-1H-pyrazol-1-yl)-1,3,5-triazin-2-amine (**3a**). After that, it was subjected to hydrazinolysis to produce N-(4-bromophenyl)-4-(3,5-dimethyl-1H-pyrazol-1-yl)-6-hydrazinyl-1,3,5-triazin-2-amine (**4a**) in a good yield (93%-99%). The target compounds **A1-3** were prepared from the condensation of **4** with different aldehydes under mild conditions. Besides, **3a** underwent substituted reaction with the amines as indicated in Table 1 to furnish target compounds **A4-12**. Compounds **B1-13** and **C1-23** were synthesized with similar procedure.

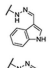
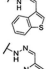
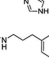
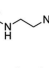
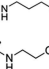
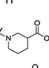
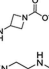
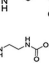
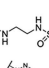
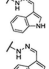
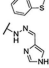
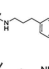
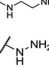
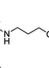
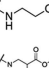
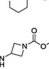
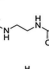
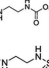


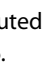


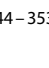

Compounds **A13-26** were synthesized as outlined in Scheme 2. Different 3,5-dimethyl-1H-pyrazole derivatives were used to substitute the chlorine atom at the 3-position of **2a** with diisopropylethylamine as base, which provided intermediate **5**. Compound **6** (**A20-23**) was easily obtained with 85% hydrazine hydrate at room temperature. Subsequently, imidization of compound **6** by indole-3-carboxaldehyde in the presence of acetic acid gave rise to **A13**. Compounds **A14-19** were synthesized with similar procedure. The two chlorine atom



Scheme 1. Synthesis of target compounds **A1-12**, **B1-13** and **C1-23**. a) NaHCO_3 , 4-bromoaniline, room temperature, 3 hrs; b) 3,5-dimethyl-1H-pyrazole, DIPEA, 120 °C, 10 hrs; c) 85% hydrazine hydrate, room temperature; d) R^2H , DIPEA, EtOH, room temperature, overnight; e) Aldehyde, AcOH, MeOH, reflux, 5 min.

Table 1. Structures of **A1** derivatives (**A1-A12**, **B1-B13**), and their IC_{50} values against the proliferation of human non-small cell lung cancer A549 and breast cancer SK-BR-3 cell lines.



Compd	R ¹	R ²	A549 ($IC_{50} \pm SD$, μM)	SK-BR-3 ($IC_{50} \pm SD$, μM)
A1(X66)	4-Br		6.1 \pm 0.6	6.0 \pm 0.05
A2	4-Br		7.4 \pm 0.2	17.6 \pm 0.6
A3	4-Br		>30	>30
A4	4-Br		5.7 \pm 0.2	16.1 \pm 2
A5	4-Br		11.0 \pm 0.9	5.2 \pm 1.0
A6	4-Br		19.8 \pm 1.8	31.4 \pm 1.7
A7	4-Br		23.4 \pm 4.6	29.1 \pm 4.8
A8	4-Br		8.9 \pm 0.6	17.8 \pm 1.5
A9	4-Br		10.4 \pm 0.3	8.7 \pm 2.7
A10	4-Br		>30	>30
A11	4-Br		9.5 \pm 0.3	11.0 \pm 0.1
A12	4-Br		18.5 \pm 2.9	27.8 \pm 4.4
B1	4-OMe		7.8 \pm 3.4	7.4 \pm 1.1
B2	4-OMe		4.6 \pm 0.3	12.3 \pm 3.6
B3	4-OMe		>30	>30
B4	4-OMe		3.2 \pm 0.7	7.1 \pm 1.8
B5	4-OMe		>30	>30
B6	4-OMe		>30	>30
B7	4-OMe		28.5 \pm 0.4	19.2 \pm 6.0
B8	4-OMe		19.7 \pm 1.9	9.5 \pm 3.1
B9	4-OMe		9.7 \pm 6.1	>30
B10	4-OMe		11.2 \pm 1.1	11.0 \pm 0.3
B11	4-OMe		>30	16.0 \pm 5.2
B12	4-OMe		17.9 \pm 3.1	>30
B13	4-OMe		22.8 \pm 2.7	10.8 \pm 0.2
GM	-	-	0.3 \pm 0.1	0.05 \pm 0.01

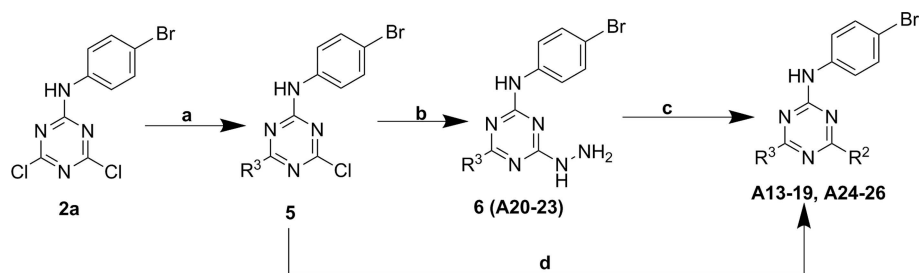
of **2a** were substituted by amines to generate corresponding compounds **A24-26**.

2.2 In Vitro Anti-Proliferative Assay

All compounds were tested for anti-proliferative activities against breast cancer SK-BR-3 (HER2 over-expressed) and non-small cell lung cancer A549 (EGFR over-expressed) cell lines by sulforhodamine B (SRB) assays. **A1** and GM were used as positive controls (Table 1). **A1-3** contained 1H-indole-3-hydrazone, benzothiothiazene-3-hydrazone and 1H-imidazole-4-hydrazone groups, respectively. The difference of activities, for **A1**, **A2**, and **A3** indicated that the type of aryl connecting hydrazone has important effect on the activities. While phenylpropylamino-substituted derivative **A4** has similar potency against A549 cells to its precursor (**A1**), its potency against SK-BR-3 cells decreases. However, ethylenediamino-substituted derivative **A5** has opposite activities against these two cell lines compared to **A4**, which suggested that the categories of R² could affect cytotoxicity. To further confirm the effects of the substituents in the position of R², seven subseries of derivatives **A6**, **A7**, **A8**, **A9**, **A10**, **A11**, **A12** were synthesized and assessed for anti-proliferative activity. Compared to lead compound **A1**, none of these compounds exhibited better anti-proliferative activities.

In order to find promising Hsp90 inhibitor, further structural optimizations were carried out. Replacement of a bromine atom (**A1**) at the C-4 position of benzene with a methoxy group (**B1**) did not increase potency significantly. Methoxy-substituted derivatives (**B7-13**) exerted moderate anti-proliferative activities like corresponding bromine-substituted derivatives (**A6-12**). Moreover, introducing benzothiothiazene-3-hydrazone and phenylpropylamino gave **B2** and **B4**, which were more potent than their precursors **A2** and **A4** against A549 cells. It is noteworthy that **B9** and **B12** can selectively inhibit A549 cells, but show lower anti-proliferative activity against SK-BR-3 cells.

Varying the methoxy group (**B1**) to a chlorine atom at the C-4 position of benzene along with a trifluoromethyl installed at the C-3 position of benzene (**C1**) did not raise anti-proliferative activity significantly (Table 2). 3-Trifluoromethyl-4-chlorine-substituted derivatives **C2**, **C4**, and **C13** were less potent than their precursors **B2**, **B4**, and **B13** respectively. Interestingly, the selectivity of **C4** towards A549 cells was enhanced. Apparently, **C3** bearing 1H-imidazole-4-hydrazone and **C11** containing acetylenediamino lost anti-proliferative activities. Besides, other 3-trifluoromethyl-4-chlorine-substituted derivatives of **C5-9** and **C12** displayed more powerful inhibitory activities than the corresponding 4-methoxy-substituted derivatives (**B5-9**, **B12**). Especially, **C6** selectively inhibited SK-BR-3 cells and had increased anti-proliferative activity against SK-BR-3 than the forerunner **A1**. The selectivity of **C4** and **C6** towards the A549 and SK-BR-3 cell lines is opposite, which may be caused by the steric hindrance of phenylpropylamino of **C4**. Substituted hydrazinyl derivatives **C14** and **C15** were designed and synthesized. These two compounds exhibited lower anti-proliferative activity against SK-BR-3 cells than **A1**. When R² is 2-(1H-pyrazol-1-yl) ethylamino, the 3-trifluoromethyl-4-chlorine-substituted derivative (**C16**) showed lower anti-proliferative activity than **A1**. **C17**, with 1-methylpiperazinyl as R², had increased anti-proliferative activity than



Scheme 2. Synthesis of target compounds **A15-26**. a) R^3H , DIPEA, 120°C, 10 hrs; b) 85% hydrazine hydrate, room temperature; c) Indole-3-carboxaldehyde, AcOH, MeOH, reflux, 5 min; d) R^2H , DIPEA, EtOH, room temperature, overnight.

Table 2. Structures of **A1** derivatives (**C1-C23**), and their IC_{50} values against the proliferation of human non-small cell lung cancer A549 and breast cancer SK-BR-3 cell lines.

Compd	R ¹	R ²	A549 ($IC_{50} \pm SD$, μM)	SK-BR-3 ($IC_{50} \pm SD$, μM)
C1	3-CF ₃ -4-Cl		11.9 ± 3.2	9.2 ± 0.3
C2	3-CF ₃ -4-Cl		9.7 ± 1.2	15.7 ± 1.4
C3	3-CF ₃ -4-Cl		>30	>30
C4	3-CF ₃ -4-Cl		10.2 ± 3.5	>30
C5	3-CF ₃ -4-Cl		7.9 ± 2.4	4.9 ± 0.7
C6	3-CF ₃ -4-Cl		29.1 ± 0.5	4.5 ± 0.6
C7	3-CF ₃ -4-Cl		15.7 ± 2.0	15.6 ± 0.3
C8	3-CF ₃ -4-Cl		15.4 ± 0.5	8.5 ± 3.0
C9	3-CF ₃ -4-Cl		9.7 ± 0.2	13.9 ± 4.4
C10	3-CF ₃ -4-Cl		13.3 ± 1.8	6.5 ± 1.6
C11	3-CF ₃ -4-Cl		>30	>30
C12	3-CF ₃ -4-Cl		14.4 ± 0.7	11.0 ± 1.7
C13	3-CF ₃ -4-Cl		26.0 ± 7.1	17.7 ± 2.1
C14	3-CF ₃ -4-Cl		7.2 ± 1.2	28.4 ± 6.2
C15	3-CF ₃ -4-Cl		8.2 ± 0.3	14.7 ± 2.6
C16	3-CF ₃ -4-Cl		10.6 ± 1.7	11.0 ± 0.8
C17	3-CF ₃ -4-Cl		5.1 ± 0.4	4.3 ± 0.4
C18	3-CF ₃ -4-Cl		8.6 ± 0.4	11.9 ± 2.3
C19	3-CF ₃ -4-Cl		7.8 ± 0.6	15.4 ± 1.6
C20	3-CF ₃ -4-Cl		8.8 ± 1.8	3.0 ± 0.5
C21	3-CF ₃ -4-Cl		5.0 ± 0.7	9.4 ± 0.9
C22	3-CF ₃ -4-Cl		4.8 ± 0.5	12.2 ± 0.6
C23	3-CF ₃ -4-Cl		8.7 ± 0.6	12.6 ± 1.0
GM	-	-	0.3 ± 0.1	0.05 ± 0.01

A1. Additionally, five aromatic amino and its derivatives (**C18-22**) were synthesized, which had moderate activities against A549 and SK-BR-3 cell lines. It was important to note that **C20**

containing 4-methoxyanilino at position of R^2 showed better anti-proliferative activity towards SK-BR-3 cells than **A1**. **C23** bearing propylamino at position of R^2 showed lower activities in both two cell lines than **A1**.

After the above structural optimization, anti-proliferative activities didn't increase much. It's necessary to change the 3,5-dimethylpyrazole motif on the scaffold (Table 3). Replacing the 3,5-dimethylpyrazolyl of **A1** with imidazolyl, morpholinyl and 2-methylimidazolyl, respectively, to give corresponding compounds **A13**, **A14** and **A15**, which turned out to be superior to

Table 3. Structures of **A1** derivatives (**A13-A26**), and their IC_{50} values against the proliferation of human non-small cell lung cancer A549 and breast cancer SK-BR-3 cell lines.

Compd	R ³	R ²	A549 ($IC_{50} \pm SD$, μM)	SK-BR-3 ($IC_{50} \pm SD$, μM)
A13			5 ± 0.6	5.7 ± 0.4
A14			2.7 ± 0.4	6.4 ± 0.1
A15			3.7 ± 0.6	5.9 ± 0.9
A16			11.6 ± 0.8	12.2 ± 0.1
A17			11.7 ± 0.9	9.3 ± 2.1
A18			15.7 ± 1.6	12.1 ± 1.1
A19			11 ± 1.5	9.0 ± 1.0
A20			>30	>30
A21			>30	12.8 ± 5.2
A22			>30	>30
A23			>30	>30
A24			16.1 ± 1.3	22.5 ± 0.1
A25			14.9 ± 1.1	20.4 ± 6.0
A26			19.7 ± 1.4	25.3 ± 4.1
GM	-	-	0.3 ± 0.1	0.05 ± 0.01

A1 in SK-BR-3 and A549 cells proliferative inhibition. However, shifting the 3,5-dimethylpyrazole motif of **A1** to aniline (**A16**), benzylamine (**A17**), phenethylamine (**A18**), and propylamine (**A19**) resulted in no substantial effects on cytotoxicity against SK-BR-3 and A549 cell lines. Changing the 3-(hydrazonomethyl)-1H-indole motif of **A1** to hydrazine, meanwhile converting the 3,5-dimethylpyrazole motif of **A1** into aniline (**A20**), 2-methylimidazole (**A21**), benzylamine (**A22**), and propylamine (**A23**) led to significant decrease of activity. Varying R^3 and R^2 to these groups, compounds **A24–26** had diminished potency.

Taken together, our results clearly indicated that the 4-bromine-substituted derivatives **A13**, **A14**, **A15** and 3-trifluoromethyl-4-chlorine-substituted derivatives **C17**, showed superior inhibition towards human breast cancer SK-BR-3 and non-small cell lung cancer A549 cell lines than **A1**. In particular, **A14** possessed the best activities against A549 cell lines.

2.3 Structure–Activity Relationships of Target Compounds

Summary of the structure–activity relationships (SARs) for synthesized compounds was depicted in Figure 2. Varying the

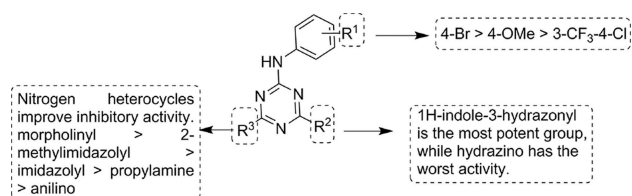


Figure 2. Summary of the structure–activity relationships of Hsp90 inhibitors.

R^3 substituents into other nitrogen heterocycles (**A13**, **A14**, **A15**) improved the anti-proliferative activity. When R^1 was substituted by 4-Br, 4-OMe and 3- CF_3 -4-Cl, the order of activities was 4-Br > 4-OMe > 3- CF_3 -4-Cl. As for R^2 , 1H-indole-3-hydrazonyl (**A13**, **A14**, **A15**) was the most potent group, while hydrazino substituted compounds (**B6**, **A20–23**) had the worst activities. We speculated that hydrazino was too small to fit the pocket well. Besides, when R^2 was substituted by acetamino ethylamino, the activities of **A10**, **B11** and **C11** were almost lost, which may be caused by poor cell membrane permeability.

2.4 The Degradation of Hsp90 Client Protein HER2

Hsp90 client protein degradation is a symbol of Hsp90 inhibitors.^[19] We tested the effects of the new compounds on client protein in HER2 over-expressed SK-BR-3 cells by western blot assay. GM was used as the positive control. Among them, compounds **A2**, **A5**, **A10**, **A13**, **A14**, **A15**, **A16**, **A17**, **A18**, **A19**, **A20**, **A22**, **A23**, **A24**, **A25**, **B1**, **B2**, **B13**, **C3**, **C5**, **C6**, **C11**, **C12**, **C13**, **C14**, **C15**, **C16**, **C17**, **C19**, **C20**, **C21**, **C22**, **C23** and **A1** treatment obviously reduced the expression of HER2 (Figure 3). Classical Hsp90 inhibitors could induce the significant HSR and the up-regulation of HSPs including Hsp72 and Hsp27.^[17,20] The

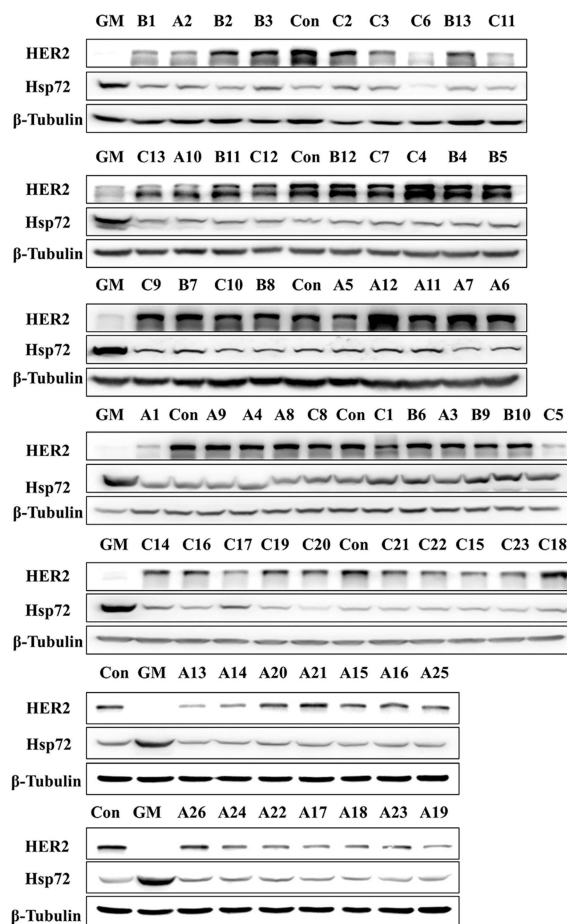


Figure 3. The effect of the new compounds on HER2/Hsp72 and their binding to Hsp90. SK-BR-3 cells were treated with the compounds (20 μ M) for 12 h, then the cells were harvested and lysed for western blot assay.

reduction of Hsp90 client proteins was usually concurrent with an induction of Hsp72, a hallmark of Hsp90 inhibition that slows down the further development of the existing Hsp90 inhibitors.^[21] Our assay showed that Hsp72 was induced by GM, but not by all these tested compounds in SK-BR-3 cells (Figure 3), which was consistent with that of the previous study of **A1**.^[15]

2.5 Compounds **A13**, **A14** and **A15** Exhibit Potent Ability of Inducing Autophagy and Cytotoxicity

Further bioassay revealed that compounds **A13**, **A14**, **A15** induced obvious autophagy in both lung cancer A549 and breast cancer SK-BR-3 cell lines at the concentration of 3 μ M, while little autophagy was induced by **A1** even at the concentration of 10 μ M (Figure 4A). To further validate whether the compounds can induce autophagy, the specific autophagy biomarker microtubule-associated protein 1A/1B-light chain 3 (LC3) was tested. The result showed an increased LC3-phosphatidylethanolamine conjugate (LC3-II) expression after treatment with **A13**, **A14** and **A15** in both A549 and SK-BR-3 cell lines, further confirming that the compounds did induce

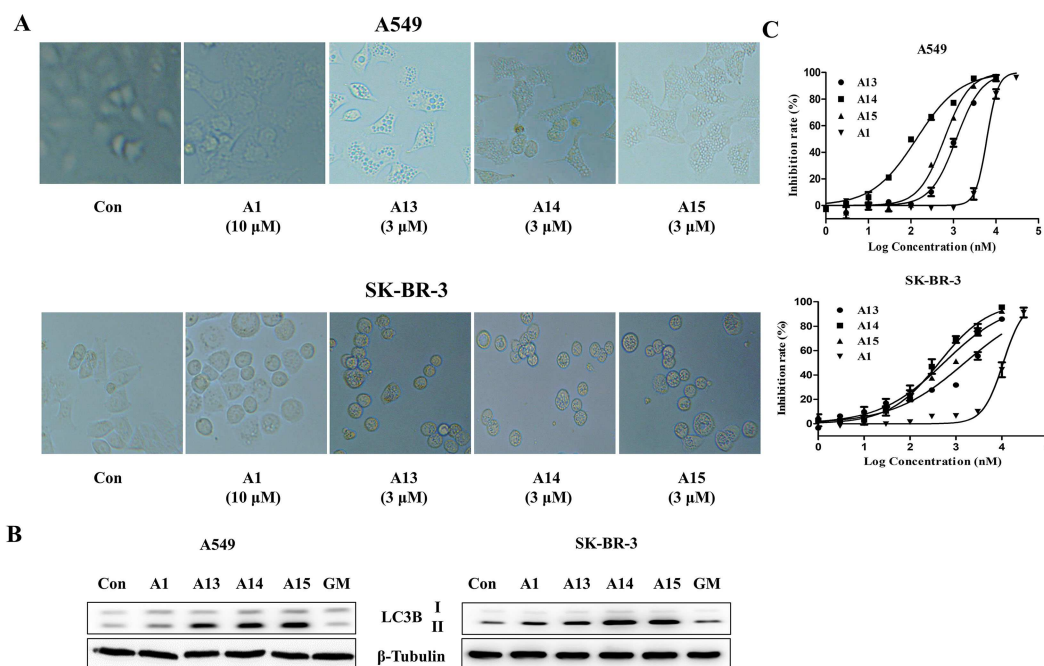


Figure 4. The effect of compounds on autophagy. (A) The effect of compounds on autophagy was observed under the microscope. (B) A549 and SK-BR-3 cells were treated with A1 (10 μM), A13, A14, A15 (3 μM), GM (1 μM) for 20 h. Whole-cell lysates were analyzed by Western blotting using the indicated antibodies. (C) A549 and SK-BR-3 cells were treated with increasing concentration of compounds for 120 h. $n = 3$; Error bars \pm SD.

autophagy (Figure 4B). Taking this result into consideration, we prolonged the exposure of the cells to the compounds for 120 h. Compared with that of 72 h treatment, the IC_{50} values of A13, A14, A15 were significantly decreased (Figure 4C, Table 3, Table 4). The IC_{50} values of A13, A14, A15 were 1.25 μM , 0.1 μM ,

Table 4. The IC_{50} values of A13, A14, A15 and A1 against A549 and SK-BR-3 cell lines for 120 h.

Compd	A549 ($\text{IC}_{50} \pm \text{SD}$, μM)	SK-BR-3 ($\text{IC}_{50} \pm \text{SD}$, μM)
A13	1.2 \pm 0.01	1.6 \pm 0.01
A14	0.1 \pm 0.02	0.4 \pm 0.01
A15	0.6 \pm 0.01	0.6 \pm 0.1
A1	6.1 \pm 0.6	10.8 \pm 1.3

0.6 μM for A549 cells and 1.6 μM , 0.4 μM , 0.6 μM for SK-BR-3 cells, respectively. The anti-proliferative activities of A13, A14, A15 were increased 3.6, 14.9, 10.7 folds in A549 cells and 4.3, 20.4, 6.1 folds in SK-BR-3 cells, respectively. However, A1 remained same anti-proliferative activity after prolonging exposure time to 120 h as that of 72 h. Above all, we supposed that autophagy induced by A13, A14 and A15 may enhance their anti-proliferative activity in cancer cell lines.

2.6 Compound A14 is a Potent Hsp90 Inhibitor

According to the above result, compound A14 had the most potent cytotoxicity and thus was chosen for further study. Hsp90 inhibitors in clinical trial, binding to ATP pocket of N-

terminal domain, inhibit Hsp90 ATPase activity and result in the degradation of oncogenic client proteins.^[21–23] Surface plasmon resonance (SPR), a technique applied to determine the affinity of two ligands,^[24] was employed to test whether these compounds bound to Hsp90 protein directly. As shown in Figure 5A, A14 bound to the recombinant human full-length Hsp90 α immobilized on sensor chip in a concentration-dependent manner with the dissociation constants (K_D) of 219 nM, while the K_D of A1 and GM are 5.3 μM and 81.3 nM.^[15] Polarization (FP) assay,^[25] a classical method of screening Hsp90 inhibitors binding to the ATP pocket, was employed. As shown in Figure 5B, similar to A1, A14 failed to compete with FITC-GM to bind to the recombinant human full-length Hsp90 α . These results indicated that A14 might bind to the site of Hsp90 α which was different from that of GM. Thus, A14 bound to the different sites of Hsp90 protein from traditional Hsp90 inhibitors and inhibited the function of Hsp90.

For a new inhibitor of Hsp90 α , it is compulsory to identify its inhibitory profile of Hsp90 client proteins as it is the molecular signature of well-known Hsp90 inhibitors. Compound A14 treatment reduced the level of HER2 and other client proteins including AKT, RAF-1, CDK4 and CDK6 in a concentration-dependent manner in SK-BR-3 cells, and had no influence on non-client protein ERK (Figure 5C). However, unlike traditional Hsp90 inhibitor, there was no concomitant activation of Hsp72 by A14. Meanwhile, the LC3-II was induced also in a concentration-dependent manner (Figure 5C). The increase of LC3-II expression suggested induction of autophagy. The mechanism between inhibition of Hsp90 function and induction of autophagy by A14 will be investigated in the future.

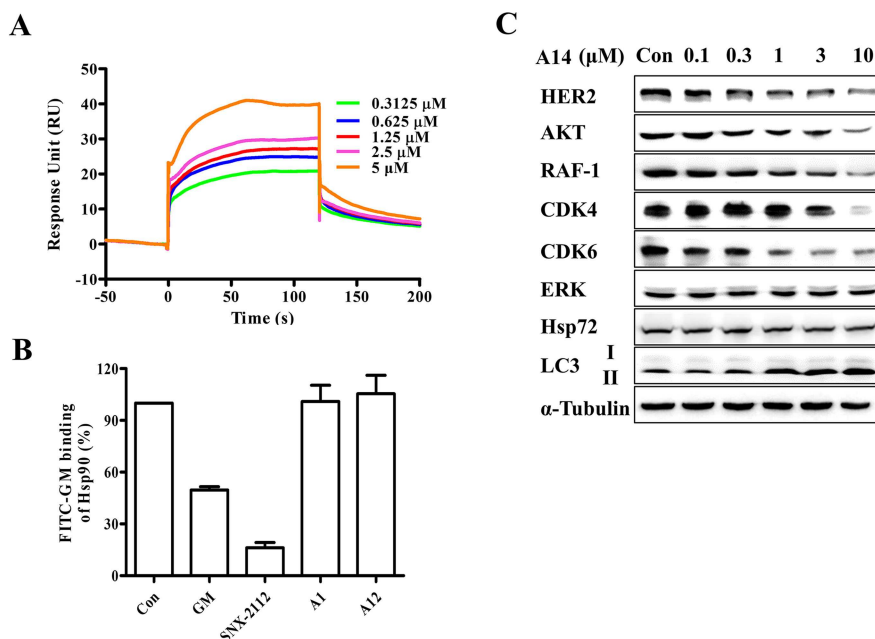


Figure 5. Identification and characterization of compound **A14** as a potent Hsp90 α inhibitor. (A) SPR analysis of **A14** binding to full-length Hsp90 α . Sensorgrams obtained by injection of **A14** in a concentration-dependent manner on immobilized Hsp90 α . (B) **A14** competed with FITC-GM using FP assay. SNX for SNX-2112. $n = 3$; Error bars \pm SD. (C) Western blot analysis of SK-BR-3 following 12 h exposure to increasing concentrations of **A14**.

2.7 In Vitro Liver Microsomal Stability Assessment of A14

In vitro metabolic stability of compound **A14** was measured using mouse, rat and human liver microsomal models (Table 5). Compound **A14** was stable in rat and human liver microsomes.

Table 5. Microsomal stability of A14					
Species	$T_{1/2}$ (min)	CL_{int} <i>in vitro</i> (mL/min/gprot) ^a	CL_{int} <i>in vivo</i> Extpl (ml/min)	CL_{int} hep <i>in vivo</i> Extpl (ml/min) ^b	MF (%) ^c
human	∞	0.00	0.00	0.00	100
rat	63.3	33.2	14.9	8.55	57.2
mouse	11.9	176.8	11.93	2.40	20.1

^a CL: clearance; ^b CL_{int} hep: hepatic clearance; ^c MF(%): metabolic bioavailability.

2.8 In Vivo Antitumor Activity of A14 Against Tumor Xenografts

Given its encouraging activity *in vitro*, we tested the anti-tumor efficacy of **A14** *in vivo*. First, the pharmacodynamics of **A14** in EGFR-positive A549 lung cancer xenografts was tested. As shown in Figure 6A and Figure 6B, following treatment with a single 70-mg/kg dose, the Hsp90 client proteins EGFR and AKT were inhibited in tumor tissues in a time-dependent manner, whereas Hsp72 was not induced. Furthermore, the expression of LC-3II, a well-known autophagy marker, was increased in tumor tissues by the treatment of **A14**.

Next, the antitumor activity of intraperitoneally (i.p.) administered **A14**, given daily, was evaluated in A549 xenografts. **A14** at a dose of 70 mg/kg inhibited tumor growth by 45% ($p < 0.01$) on the final treatment day (Figure 6D). These treatments were well tolerated, as evidenced by the absence of significant body weight loss during the course of the experiment in all groups (Figure 6C). Consistent with *in vitro* results, the treatment of **A14** caused a decrease of Hsp90 client proteins HER2 and AKT in tumor tissue (Figure 6E, Figure 6F). And there was a significant increase of LC-3II and no induction of Hsp72. Taken together, **A14** exhibited target inhibition in tumor tissues and anti-tumor activity against EGFR-positive A549 lung cancer xenografts.

3. Conclusions

Based on our previously reported Hsp90 inhibitor discovered by virtual screening, a novel series of triazine derivatives were successfully designed, synthesized in this study. The newly synthesized structures were characterized by ^1H NMR, ^{13}C NMR and mass spectrometry. All compounds are evaluated as Hsp90 inhibitors with potent anti-proliferative activity and degradation of Hsp90 client proteins. Several compounds directly bind to Hsp90, cause Hsp90 client proteins degradation and result in inhibition of tumor cell proliferation. Compounds **A13**, **A14**, **A15** induce significant autophagy and exhibit potent anti-tumor activity in HER2 overexpressed SK-BR-3 and EGFR overexpressed A549 cell lines. Additionally, the most potent compound **A14**, characterized as a novel Hsp90 inhibitor, binds to the N-terminal domain of Hsp90 that is different from traditional Hsp90 inhibitors like GM. Remarkably, **A14** induces degradation

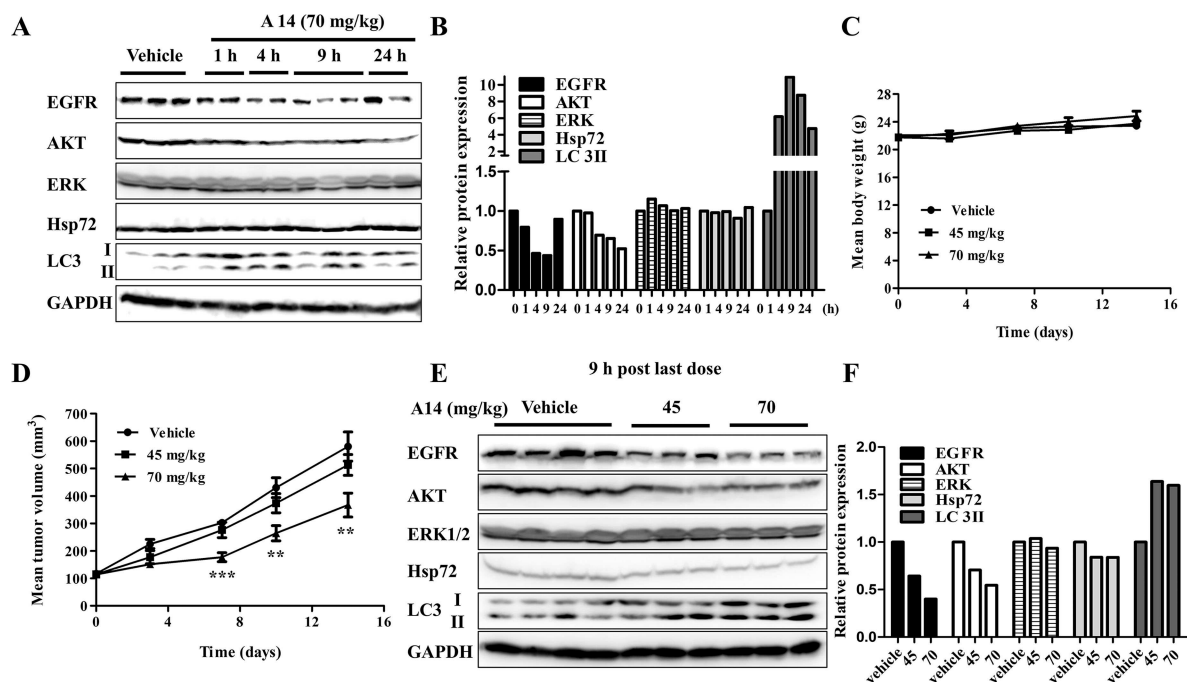


Figure 6. *In vivo* study of A14. (A) pharmacodynamics study of A14. A549 tumor-bearing mice were administered a single 70-mg/kg dose of A14. Tumor extracts were analyzed in parallel by Western blotting. (B) The quantification analysis of protein expression. (C) A549 tumor-bearing mice were administered A14 (i. p.) daily for 14 days. Tumor volumes were measured twice a week. (D) The body weight of mice was measured twice a week. (E) Mice were sacrificed 9 h after the last dose, and tumors were removed and analyzed by Western blotting. (F) The quantification analysis of protein expression.

of client proteins, but does not accompany increase of Hsp72. Compared with lead compound A1 ($K_D = 5.3 \mu\text{M}$; $IC_{50} = 6.1 \sim 10.8 \mu\text{M}$), the ability of A14 binding to Hsp90 ($K_D = 0.219 \mu\text{M}$), Hsp90 inhibitory activity and the anti-tumor activity ($IC_{50} = 0.1 \sim 0.4 \mu\text{M}$) are significantly improved. Also, A14 exhibited *in vivo* anti-tumor activity against EGFR-positive A549 lung cancer xenografts. Taken together, the unique pharmaceutical properties demonstrated the compound A14 is a novel and promising lead of Hsp90 inhibitor. This study provides insights into the evolution of Hsp90 inhibitors and may facilitate the design of new Hsp90 inhibitor for the antitumor drug development without induction of heat shock response to overcome the drawback caused by traditional Hsp90 inhibitors.

Experimental Section

General Information and Materials. All starting materials and solvents were purchased from commercial suppliers and used without further purification. Reactions were monitored by thin layer chromatography (TLC) of silica gel (HSGF254) at 254 nm wavelength. The LRMS and HRMS were recorded on Finnigan LCQ/DECA and Micromass Ultra Q-TOF (ESI) spectrometer, respectively.

The ^1H and ^{13}C spectra were taken on Bruker Avance - 400 and 500 NMR spectrometer operating at 400 or 500 MHz for ^1H and 125 MHz for ^{13}C NMR, respectively, using TMS as the internal standard and CDCl_3 or $\text{DMSO}-d_6$ as the solvent. Chemical shifts are given in δ values of ppm. The abbreviations s is singlet, d is doublet, t is triplet and m is multiplet. Coupling constants (J) were measured in hertz (Hz).

All target compounds and their intermediates in CDCl_3 or $\text{DMSO}-d_6$ exhibited special signals in ^1H and ^{13}C spectrums, which may be due to the structural resonance. They are indicated with *major* or *minor*. The purity ($\geq 95\%$) of new synthesized compounds was verified by the HPLC study performed on Agilent C18 (4.6 mm \times 250 mm, 5 μm) column using a mixture of solvent methanol/water at a flow rate of 1 mL/min and monitoring by UV absorption at 254 nm.

N-(4-bromophenyl)-4,6-dichloro-1,3,5-triazin-2-amine (2a): The solution of 4-bromoaniline (4.66 g, 0.027 mol) in THF (50 ml) was added dropwisely into a solution of 2,4,6-trichloro-1,3,5-triazine (5.0 g, 0.027 mol) and NaHCO_3 (4.56 g, 0.054 mol) in dry THF (50 ml) at 0°C . Then the reaction mixture was allowed to warm to room temperature and stirred for 3 hours. After that the reaction mixture was filtered and the filtrate was concentrated under reduced pressure. The residue was dispersed in petroleum ether and the mixture was then filtered to afford a pale yellow powder (8.1 g, 93.1% yield). ^1H NMR (400 MHz, CDCl_3) δ 7.60 (s, 1H), 7.57–7.52 (m, 2H), 7.49–7.44 (m, 2H). ^{13}C NMR (125 MHz, $\text{DMSO}-d_6$) δ 170.14, 169.26, 164.15, 136.84, 132.18, 123.70, 117.36. HRMS (ESI): calcd. for $\text{C}_9\text{H}_6\text{N}_4\text{BrCl}_2$ [$M + \text{H}$] $^+$: 318.9153, found: 318.9149.

N-(4-bromophenyl)-4-chloro-6-(3,5-dimethyl-1H-pyrazol-1-yl)-1,3,5-triazin-2-amine (3a, major; minor = 52: 48): DIPEA (1.74 ml, 11.8 mmol) and 3,5-dimethyl-1H-pyrazole (0.53 g, 5.5 mmol) were added into a solution of compound 2 (1.90 g, 5.9 mmol) in dioxane (30 mL), respectively. Then the reaction mixture was allowed to stir at 120°C for 10 hours. After that, the reaction mixture was concentrated and the residue was dispersed in water, filtered and the solid was dried in vacuum drier. Finally, the solid was recrystallized in petroleum ether/dioxane (5:1) to give a white powder (1.85 g, 82.2% yield). ^1H NMR (400 MHz, $\text{DMSO}-d_6$) δ 10.95 (s, 1H, minor), 10.92 (s, 1H, major), 7.69–7.63 (m, 2H), 7.58 (d, $J = 8.5$ Hz, 2H), 6.24 (s, 1H), 2.63 (s, 1H, minor), 2.52 (s, 1H, major), 2.21 (s, 3H).

HRMS (ESI): calcd. for $C_{14}H_{13}BrClN_6$ $[M+H]^+$: 380.9995, found: 380.9991.

Compound **5** was prepared using the same procedure as that for **3a** and used directly in the next reaction without purification.

N-(4-bromophenyl)-4-(3,5-dimethyl-1H-pyrazol-1-yl)-6-hydrazinyl-1,3,5-triazin-2-amine (4a, major: minor=57: 43): The solution of compound **3a** (3.8 g, 10 mmol) in ethanol (200 ml) was added into the solution of 85% hydrazine hydrate (0.29 ml, 50 mmol) in ethanol (50 ml). After stirring overnight at room temperature, the reaction mixture was concentrated and then the residue was washed by water, dried by vacuum drier to afford a white solid which was directly used in the next step without further purification (3.75 g, 100% yield). 1H NMR (400 MHz, $DMSO-d_6$) δ 10.01 (s, 1H), 8.96 (s, 1H, major), 8.89 (s, 1H, minor), 7.83 (d, $J=9.3$ Hz, 2H), 7.45 (t, $J=8.9$ Hz, 2H), 6.13 (s, 1H, minor), 6.10 (s, 1H, major), 4.43 (s, 2H), 2.67 (s, 3H, major), 2.58 (s, 3H, minor), 2.18 (s, 3H, minor), 2.17 (s, 3H, major). ^{13}C NMR (125 MHz, $DMSO-d_6$) δ 168.33, 165.03 (major), 164.40 (minor), 163.30 (minor), 162.79 (major), 150.17 (minor), 149.82 (major), 143.56 (minor), 142.98 (major), 139.76 (minor), 139.48 (major), 131.65 (major), 131.59 (minor), 122.66 (minor), 122.12 (major), 114.38 (major), 114.13 (minor), 110.56 (minor), 110.23 (major), 16.08 (minor), 15.56 (major), 13.88. HRMS (ESI): calcd. for $C_{14}H_{16}N_8Br$ $[M+H]^+$: 375.0681, found: 375.0677.

Compound **6** was prepared using the same procedure as that for **4a** and used directly in the next reaction without purification.

4-(2-((1H-indol-3-yl)methylene)hydrazinyl)-N-(4-bromophenyl)-6-(3,5-dimethyl-1H-pyrazol-1-yl)-1,3,5-triazin-2-amine (A1, major: minor=71: 29): Acetic acid (10 ml) was added into the solution of compound **4** (3.75 g, 10 mmol) and indole-3-aldehyde (1.45 g, 10 mmol) in methanol (70 ml). The reaction mixture was refluxed for 5 minutes. Upon cooling, a white precipitate was formed, then the mixture was filtered and the solid was washed by methanol to produce the compound **A1** as a white powder (4.4 g, 87.6% yield). 1H NMR (400 MHz, $DMSO-d_6$) δ 11.60 (s, 1H, major), 11.55 (s, 1H, minor), 11.50 (s, 1H, major), 11.27 (s, 1H, minor), 10.15 (s, 1H), 8.54–8.34 (m, 2H), 8.27–7.74 (m, 3H), 7.64–7.37 (m, 3H), 7.39–7.03 (m, 2H), 6.20 (s, 1H, minor), 6.15 (s, 1H, major), 2.92 (s, 3H, minor), 2.69 (s, 3H, major), 2.22 (s, 3H, minor), 2.20 (s, 3H, major). ^{13}C NMR (125 MHz, $DMSO-d_6$) δ 165.14 (major), 164.79 (minor), 164.39, 163.77 (minor), 163.15 (major), 150.27 (minor), 150.05 (major), 143.59 (minor), 143.19 (major), 142.83, 139.88 (minor), 139.72 (major), 137.66 (major), 137.46 (minor), 131.67 (minor), 131.57 (major), 130.90 (major), 130.52 (minor), 124.71, 123.17 (major), 123.06 (minor), 122.57 (minor), 122.44 (major), 122.23, 120.54, 114.32 (major), 114.23 (minor), 112.42 (major), 112.26 (minor), 110.62 (minor), 110.42 (major), 15.94 (minor), 15.70 (major), 13.97 (minor), 13.90 (major). HRMS (ESI): calcd. for $C_{23}H_{21}N_9Br$ $[M+H]^+$: 502.1103, found: 502.1100.

Compounds **A2-A3**, **A13-A19**, **B1-B3**, **C1-C3** were prepared using the same procedure as that for **A1**.

Cell Culture

The cancer cell lines SK-BR-3 and A549 were purchased from the American Type Culture Collection (Manassas, VA, USA). All cell lines were maintained in DMEM containing 10% fetal bovine serum at 37 °C and 5% CO_2 in a humid environment.

SRB Assay

Tumor cells were seeded in the 96-wells plates overnight and then were treated with increasing doses of compounds in triplicate for

72 h. The anti-proliferative activities were accessed by SRB assay. Then the OD was measured at 510 nm wavelength using Synergy H4 Hybrid reader (BioTek, Winooski, VT, USA) using Gen5.0 software (BioTek). The IC_{50} values were calculated using the software Prism 5 (GraphPad Software, Inc).

Western Blot Assay

After treatment with compounds, cells were washed with ice-cold phosphate-buffered saline (PBS:137 mM NaCl, 2.7 mM KCl, 10 mM Na_2HPO_4 , and 1.8 mM KH_2PO_4) and lysed in sodium dodecyl sulfate (SDS) sample buffer. Equal amount of whole cell lysates was separated by SDS-PAGE, and transferred to polyvinylidene difluoride membranes. Then blocking in 5% nonfat milk in Tris-buffered saline with 0.1% Tween-20 (pH 7.6), membranes were incubated with the appropriate primary antibodies at 4 °C overnight and then were incubated with the secondary antibodies for 2 h at room temperature. Immunoreactive proteins were visualized using an enhanced chemiluminescence system (Thermo Fisher Scientific, Waltham, MA).

FP Assay

Compounds were incubated with recombinant human full-length Hsp90 α protein for 1 h in a 96-well microplate at 4 °C in the presence of the assay buffer (20 mM HEPES, pH 7.4, 50 mM KCl, 5 mM $MgCl_2$, 20 mM $NaMoO_4$, 0.01% NP40, 2 mM DTT and 0.1 mg/mL BSA), and then incubated for 4 h after added FITC-GM. Polarization was measured in Synergy H4 Hybrid reader (BioTek).

SPR Assay

Measurements of SPR were performed as described previously.^[15] We used the biacore T200 (GE healthcare, Cleveland, OH, USA) to immobilize Hsp90 α (100 μ g/mL in 10 mM pH 4.0) on the CM5 sensor chip surface to get densities of 12000 RU. Then quenched with 1 M ethanolamine. Compounds were diluted in HBS-EP (20 mM HEPES, pH 7.4, 150 mM NaCl, 0.5 M EDTA, 0.05% P20), and injected from lowest to highest concentrations at a flow rate of 30 μ L/min for 120 seconds, and the dissociation of compound-protein complex was monitored for an additional 180 seconds for compounds **A14**.

In Vitro Liver Microsomal Stability Assessment

Microsomes in 0.1 M TRIS buffer pH 7.4 (final concentration 0.33 mg/mL), co-factor $MgCl_2$ (final concentration 5 mM) and tested compound (final concentration 0.1 μ M), co-solvent (0.01% DMSO) and 0.005% Bovin serum albumin (BSA) were incubated at 37 °C for 10 min. The reaction was started by the addition of NADPH (final concentration 1 mM). Aliquots were sampled at 0, 7, 17, 30 and 60 min respectively and methanol (cold in 4 °C) was added to terminate the reaction. After centrifugation (4000 rpm, 5 min), samples were then analyzed by LC-MS/MS.

In Vivo Study

Female Balb/cA-nude mice (5–6 wk old) were purchased from Shanghai Laboratory Animal Center, (Shanghai, China). Human tumor xenografts were prepared by subcutaneously implanting A549 cells in the right flank of the animal. When tumor volumes reached ~ 100 mm³, mice were randomly assigned to control (n=10) or treatment (n=6) groups, and treated with **A14** for 14 days. **A14** was administered daily at a dose of 45 or 70 mg/kg (i.p.) for

14 days. Tumor volume was calculated as $(\text{length} \times \text{width}^2)/2$. The therapeutic effect of a given compound was expressed in terms of tumor growth inhibition (TGI), calculated as $\text{TGI} = (V_t' - V_t) / (V_c' - V_c) \times 100\%$, where V_t' and V_t are tumor volumes in treatment groups on each day of measurement and on the day of initial treatment, respectively, and V_c' and V_c are tumor volumes in the vehicle control group on each day of measurement and on the day of initial treatment, respectively.

In pharmacodynamics studies, mice bearing A549 tumors received a single 70-mg/kg dose of **A14** or vehicle (i.p.), and tumor tissue were collected at different times. Tumor samples were analyzed by Western blotting.

Animal experiments were conducted in accordance with guidelines of the Institutional Animal Care and Use Committee at the Shanghai Institute of Materia Medica, Chinese Academy of Sciences.

Appendix A. Supporting information

Supplementary data associated with this article can be found in the online version.

Acknowledgements

This research was supported by grants from the National Key R&D Plan (2016YFA0502301), National Major Scientific and Technological Special Project for "Significant New Drugs Development" (2018ZX09711002), National Natural Science Foundation of China (N^o 81573350, 81273546, 81603270).

Conflict of Interest

The authors declare no conflict of interest.

Keywords: autophagy · Hsp72 · Hsp90 inhibitor · triazines · antitumor activity

- [4] S. Tomaselli, M. Meli, J. Plescia, L. Zetta, D. C. Altieri, G. Colombo, L. Ragona, *Chem. Biol. Drug Des.* **2010**, *76*, 382–391.
- [5] J. S. Isaacs, W. P. Xu, L. Neckers, *Cancer Cell.* **2003**, *3*, 213–217.
- [6] A. Kamal, M. F. Boehm, F. J. Burrows, *Trends Mol. Med.* **2004**, *10*, 283–290.
- [7] A. S. Sreedhar, P. Csermely, *Pharmacol. Ther.* **2004**, *101*, 227–257.
- [8] C. E. Stebbins, A. A. Russo, C. Schneider, N. Rosen, F. U. Hartl, N. P. Pavletich, *Cell.* **1997**, *89*, 239–250.
- [9] R. Bhat, S. R. Tummalaipalli, D. P. Rotella, *J. Med. Chem.* **2014**, *57*, 8718–8728.
- [10] M. Bedin, A. M. Gaben, C. Saucier, J. Mester, *Int. J. Cancer.* **2004**, *109*, 643–652.
- [11] H. Zhou, J. C. Vederas, Y. Tang, *Abstr. Pap. Am. Chem. Soc.* **2011**, *241*.
- [12] L. Wright, X. Barril, B. Dymock, L. Sheridan, A. Surgenor, M. Beswick, M. Drysdale, A. Collier, A. Massey, N. Davies, A. Fink, C. Fromont, W. Aherne, K. Boxall, S. Sharp, P. Workman, R. E. Hubbard, *Chem. Biol.* **2004**, *11*, 775–785.
- [13] R. I. Morimoto, *Genes Dev.* **1998**, *12*, 3788–3796.
- [14] R. Bagatell, G. D. Paine-Murrieta, C. W. Taylor, E. J. Pulcini, S. Akinaga, I. J. Benjamin, L. Whitesell, *Clin. Cancer Res.* **2000**, *6*, 3312–3318.
- [15] Z. X. Zhao, J. M. Zhu, H. T. Quan, G. M. Wang, B. Li, W. L. Zhu, C. Y. Xie, L. G. Lou, *Oncotarget.* **2016**, *7*, 29648–29663.
- [16] K. D. Sarge, S. P. Murphy, R. I. Morimoto, *Mol. Cell. Biol.* **1993**, *13*, 1392–1407.
- [17] R. Baler, G. Dahl, R. Voellmy, *Mol. Cell. Biol.* **1993**, *13*, 2486–2496.
- [18] C. Garrido, M. Brunet, C. Didelot, Y. Zermati, E. Schmitt, G. Kroemer, *Cell Cycle.* **2006**, *5*, 2592–2601.
- [19] D. B. Solit, G. Chiosis, *Drug Discovery Today* **2008**, *13*, 38–43.
- [20] P. W. Piper, S. H. Millson, *Pharmaceuticals* **2011**, *4*, 1400–1422.
- [21] S. A. Eccles, A. Massey, F. I. Raynaud, S. Y. Sharp, G. Box, M. Valenti, L. Patterson, A. de Haven Brandon, S. Gowan, F. Boxall, W. Aherne, M. Rowlands, A. Hayes, V. Martins, F. Urban, K. Boxall, C. Prodromou, L. Pearl, K. James, T. P. Matthews, K. M. Cheung, A. Kalusa, K. Jones, E. McDonald, X. Barril, P. A. Brough, J. E. Cansfield, B. Dymock, M. J. Drysdale, H. Finch, R. Howes, R. E. Hubbard, A. Surgenor, P. Webb, M. Wood, L. Wright, P. Workman, *Cancer Res.* **2008**, *68*, 2850–60.
- [22] K. Lundgren, H. Zhang, J. Brekken, N. Huser, R. E. Powell, N. Timple, D. J. Busch, L. Neely, J. L. Sensintaffar, Y. C. Yang, A. McKenzie, J. Friedman, R. Scannevin, A. Kamal, K. Hong, S. R. Kasibhatla, M. F. Boehm, F. J. Burrows, *Mol. Cancer Ther.* **2009**, *8*, 921–9.
- [23] T. Nakashima, T. Ishii, H. Tagaya, T. Seike, H. Nakagawa, Y. Kanda, S. Akinaga, S. Soga, Y. Shiotsu, *Clin. Cancer Res.* **2010**, *16*, 2792–802.
- [24] F. Vallee, C. Carrez, F. Pilorge, A. Dupuy, A. Parent, L. Bertin, F. Thompson, P. Ferrari, F. Fassy, A. Lambertson, A. Thomas, R. Arrebola, S. Guerif, A. Rohaut, V. Certal, J. M. Ruxer, T. Gouyon, C. Delorme, A. Jouanen, J. Dumas, C. Grepin, C. Combeau, H. Goulaouic, N. Dereu, V. Mikol, P. Mailliet, H. Minoux, *J. Med. Chem.* **2011**, *54*, 7206–19.
- [25] J. Kim, S. Felts, L. Llauger, H. He, H. Huezo, N. Rosen, G. Chiosis, *J. Biomol. Screening* **2004**, *9*, 375–81.

[1] M. Taipale, D. F. Jarosz, S. Lindquist, *Nat. Rev. Mol. Cell Biol.* **2010**, *11*, 515–528.

[2] L. Whitesell, S. L. Lindquist, *Nat. Rev. Cancer.* **2005**, *5*, 761–772.

[3] L. Neckers, P. Workman, *Clin. Cancer Res.* **2012**, *18*, 64–76.

Manuscript received: February 3, 2019

Revised manuscript received: February 28, 2019